Supporting Information

A Novel Pyrrolo[3,4-*b*]dithieno[2,3-*f*:3',2'-*h*]quinoxaline-8,10 (9H)-dione – Based medium bandgap π- conjugated polymer donor for high –performance Ternary non-fullerene Polymer Solar Cells with an Efficiency of Over 17%

M. L. Keshtov[a*], D. P. Kalinkin[a], D.Y.Shikin[a], S. M. Peregudova[a], Zh Xie[b], Ganesh D. Sharma[c]*
[a]A.N. *Nesmeyanov Institute of Organoelement compounds of the Russian Academy of Sciences, Vavilova St., 28, 119991 Moscow, Russian Federation.*
[b]*Changchun Institute of Applied Chemistry, Chinese Academy of Science, Ren Min Street, Changchun, P. R. China*
[c]*Department of Physics and Center for Material Science and Nano-Electronics, The LNM Institute for Information Technology, Jamdoli, Jaipur (Raj.) 302031, India*

Experimental Part

Instruments

^{1}H NMR spectra were obtained on Agilent 400 MHz DD2 nuclear magnetic resonance (NMR) spectrometer, using $CDCl_3$as solvent at a resonancefrequency of 600 MHz at room temperature. UV-vis absorption spectra were recorded on a Shimadzu UV-2600 spectrophotometer. The molecular weight of polymers was determined by Waters 1515 gel permeation chromatography using 1,2,4-trichlorobenzene as eluent at 60^{o}C and polystyrene as a standard. The thermogravimetric analysis (TGA) was measured on NETZSCH (DSC 200F3) at a heating rate of 10^o C/min under nitrogen atmosphere. Oxidation and reduction potentials of the compounds were determined by cyclic voltammetry (CV) experiments on a computer-controlled potentiostatAuto lab type III" at a scan rate of 100 mVs^{-1}. A platinum working electrode, Ag/Ag+ (0.1 M in anhydrous acetonitrile), and a platinum wire were used as the working electrode, reference electrode, and counter electrode, respectively, in a nitrogen-saturated solution of tetrabutylammonium hexafluorophosphate (Bu4NPF6) (0.1 M in anhydrous acetonitrile). Potential was referenced to the ferrocene/ferrocenium (Fc/Fc^+) coupled by an internal standard and was assigned as an absolute energy of -4.44 eV versus vacuum. The HOMO and LUMO energy levels were determined according to the equations: $E_{HOMO}= - q[E_{ox}+ 4.44]$ (eV), and $E_{LUMO}=- q[E_{red}+ 4.48]$ (eV), where oxidation/reduction onset potential (E_{ox}/E_{red}) was determined from the position at which the current raised initially from the baseline.

Materials

All of the reagents and chemicals were purchased from Aldrich, Acros, and TCI and used without further purification.Toluene was dried and purified by fractional distillation over sodium/benzophenone under argon. 4,8-bis(5-(2-ethylhexyl)thiophen-2-yl)benzo[1,2-b:4,5-b']dithiophene-2,6-diyl)bis (trimethylstannane) M1 [1] and 2,5-dibromo-9-(2-octyldodecyl)-8H-pyrrolo[3,4-b]dithieno [2,3-f:3',2'-h] quinoxaline-8,10 (9H)-dione M2 [2], were synthesized according to the literature procedures.

Synthesis of polymer P(BDTPtQD)

A mixture of 4,8-bis(5-(2-ethylhexyl)thiophen-2-yl)benzo[1,2-b:4,5-b']dithiophene-2,6-diyl)bis(trimethylstannane) M1 (0.4523g, 0.5 mmol),) 2,5-dibromo-9-(2-octyldodecyl)-8H-pyrrolo[3,4-b]dithieno [2,3-f:3',2'-h] quinoxaline-8,10 (9H)-dione M2(0.3748g, 0.5 mmol) and palladium catalyst $Pd(Ph_3P)_4$ (0.027g)were dissolved in dry toluene (16 ml) and refluxed under argon for 48 h while stirring. After cooling to room temperature, the reaction mixture was added dropwise with vigorous stirring to methanol to remove low molecular weight residues and oligomers. The resulting crude product was extracted in a Soxhlet apparatus with methanol, hexane and chloroform in succession. The polymer was then isolated from the chloroform fraction using a rotary evaporator as a solid black product in high yield (0.47g, 81%). Elem. Anal. Calcd for ($C_{68}H_{83}N_3O_2S_6$): C, 70.00; H, 7.17; N, 3.60; O, 2.74; S, 16.49 Found: C, 70.18; H, 7.08; N, 3.390; S, 16.11%. ^{1}H NMR ($CDCl_3$, 400 MHz, δ / ppm): 8.30-7.35 (br, 6H), 7.25-6.45 (br, 2H)(aryl), 4.30-3.75(br,2H,NCH_2-)), 3.50-2.75 (br, 4H, -CH), 2.27-0.36(br,66H)

Device fabrication and characterization

The binary and ternary devices were fabricated with a conventional structure of ITO/PEDOT:PSS/active layer/PFN-Br/Ag as the following procedures. The ITO-coated glasses were cleaned using a detergent scrub, and subsequently subjected to ultrasonic treatment in deionized water, acetone and isopropyl alcohol for 20 min in each step. After that the ITO substrates were treated with ultraviolet-ozone for 15 min and spin coated with PEDOT:PSS solution at 4000 rpm for 30 s and subsequently annealed at 120° C for 20 min under ambient conditions. We have used P137 as donor and two nonfullerene small molecule acceptors (BTP-eC9 and DBTBT-IC) as acceptor for the fabrication of OSCs. Chloroform solution with **P(BDTPtQD)**:BTP-eC9 (with different weight ratios) **P(BDTPtQD)**:DBTBT-IC (with different weight ratio) for binary devices and ternary **P(BDTPtQD)**:DBTBT-IC:BTP-eC9 with different weight ratio of DBTBT-IC and BTP-eC9 keeping concentration of P137 constant) for ternary devices were spin coated onto the PEDOT:PSS at 2500 rpm for 30 s and dried for 30 min. The total concentration for each blend was kept 16 mg/mL. Afterward, PFN-Br with concentration of

1.0 mg/mL of methanol containing 0.3 % (v/v) glacial acetic acid was spin coated on the active layer at 3000 rpm for 20 s. The optimized active layers were subjected to solvent vapor annealing under THF for 40 s, before the deposition of PFN-Br. Finally, the Ag (thickness 150 nm) was deposited under high vacuum onto PFN-Br layer. The effective area of the device is 0.04 cm^2, defined by the masks for all the OSCs.

The current-voltage characteristics of the OSCs were measured under illumination intensity of 100 mW/cm^2 (AM1.5 G) using a solar simulator (AAA model) and a Keithley 2400 source meter unit. The Solar simulator calibration is done using a calibrated reference solar cell, which outputs a standard value of 1Sun. The External quantum efficiency (EQE) measurements were performed using Bentham EQE system.

The hole-only and electron-only devices with ITO/PEDOT:PSS/active layer /Au and ITO/Al/ active layer/Al architectures were also fabricated in a similar way, to measure the hole and electron mobility. We have measured the dark J-V characteristics and fitted with the space charge limited current model using the following expression:

$J_{SCLC} = (9/8)\varepsilon\varepsilon_0\mu[(V-V_{bi})^2/L^3]$, where ε, ε_0 is the permeability of active layer and vacuum, respectively, V and Vbi are the applied voltage and built-in potential, respectively, μ is the charge carrier mobility, and L is the thickness of the active layer.

The photocurrent density (J_{ph}) and effective voltage (V_{eff}) were estimated as:

$J_{ph}= J_L-J_D$, where J_L and J_D are the photocurrent densities under illumination and in dark conditions, respectively.

$V_{eff}= V_o-V_a$, where V_o is the voltage when $J_{ph}=0$ and V_a is the applied bias voltage.

For the transient photocurrent (TPC) and transient photovoltage (TPV) decay, the device was mounted on a conductive clip under steady state illumination from the focused quartz-tungsten halogen lamp light source. An optical perturbation is applied to the device with a 1kHz femtosecond pulse laser under 500 nm excitation. The TPV signal was acquired by a digital oscilloscope at open circuit conditions (1MΩ). The TPC signal was measured under short circuit by applying a 50 resistor. The carrier lifetime and charge carrier extraction times were estimated via fitting the TPV and TPC decay with an exponential fitting.

Steady state PL spectra of the thin film was recorded on the Shimazu PL spectrophotometer.

The time resolved photoluminescence (TPRL) in the films were recorded on HORIB make.

TEM and XRD measurement details: The TEM images were taken on transmission electron

microscope (TEM, Techai F20 FEI) operated at an accelerating voltage of 200 KV. The film x-ray diffraction (XRD) patterns were collected using a Panalytical x' Pert PRO MPD diffractometer with CuKαradiation.

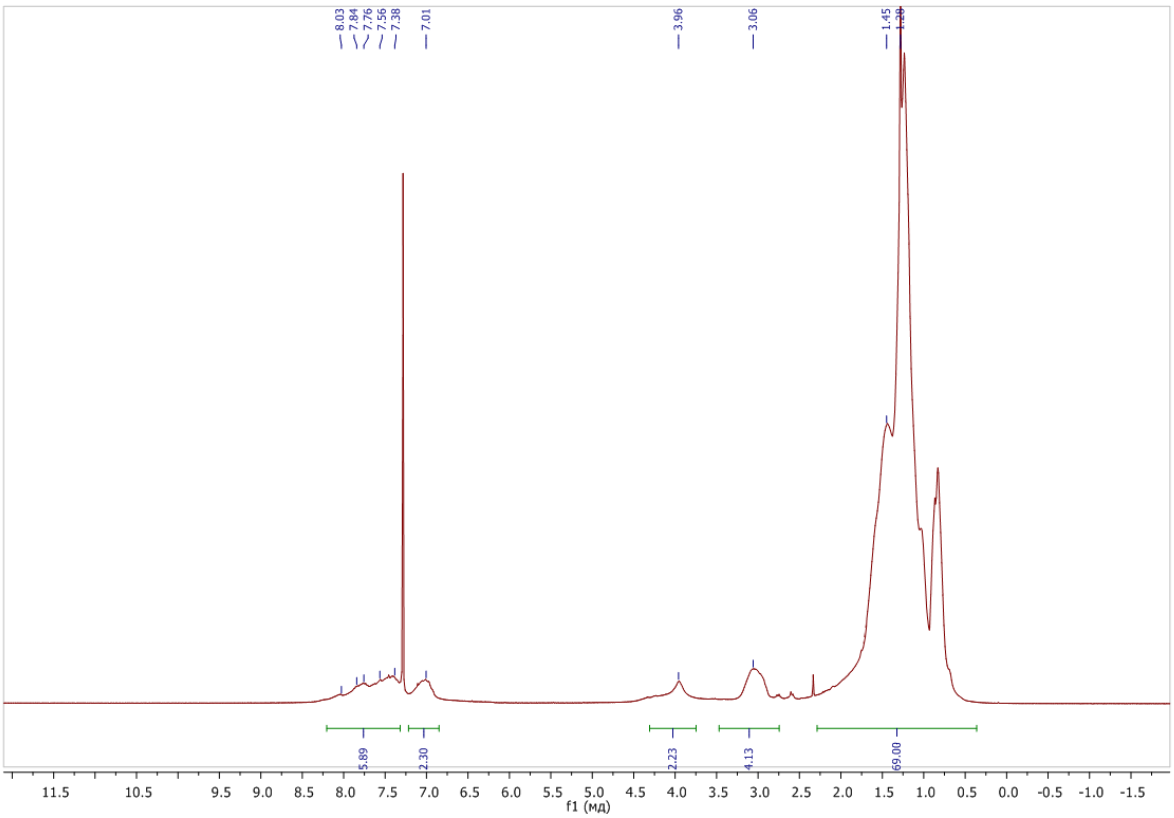

Figure S1.[1]H-NMR spectrum of copolymer **P(BDTPtQD)** in $CDCl_3$.

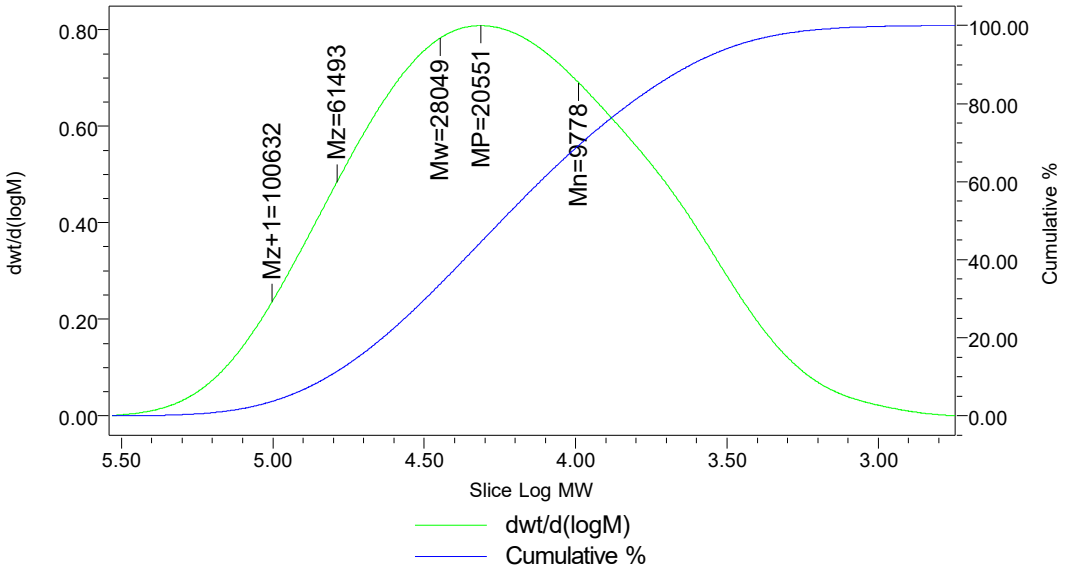

Figure S2. GPC spectra of the **P(BDTPtQD)**

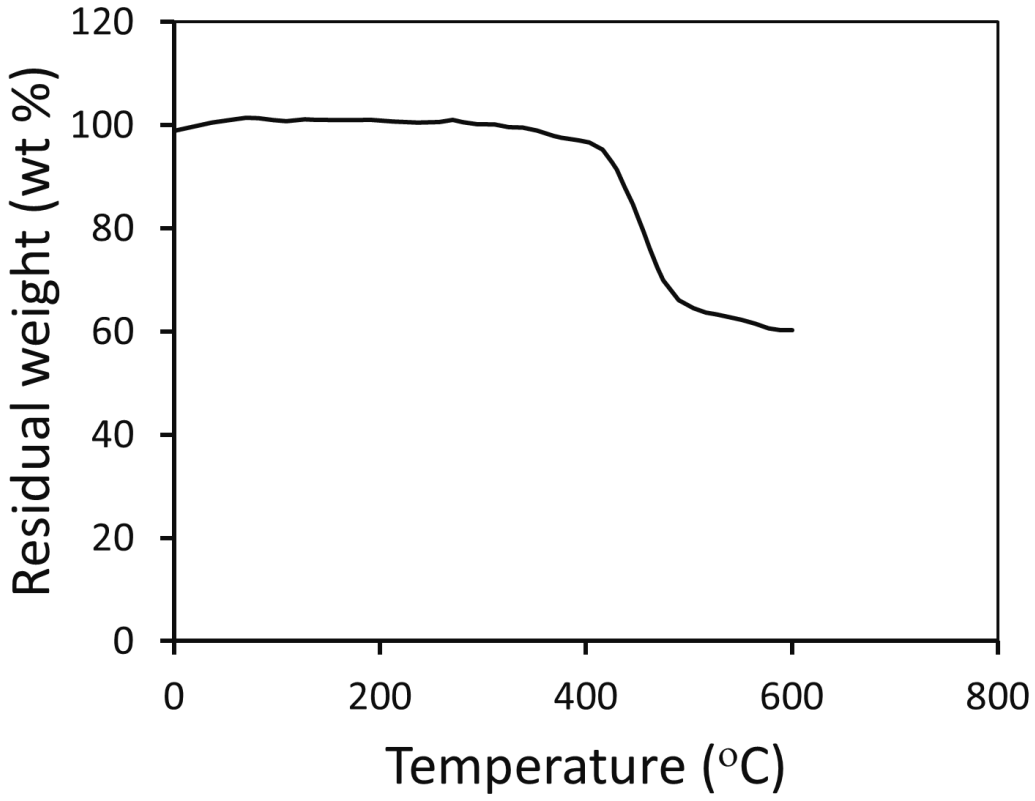

Figure S3.TGA curve of the copolymer**P(BDTPtQD)** with a heating rate of 10°C/min.

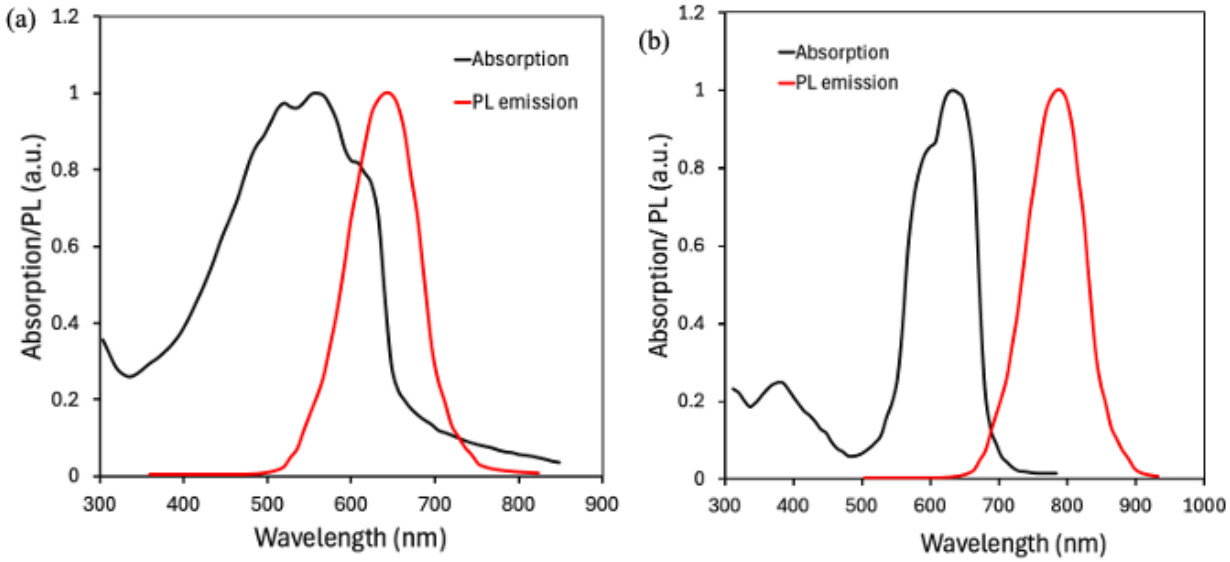

Figure S4. Normalized thin film absorption and PL spectra of the (a)**P(BDTPtQD)**and (b) PBDB-T

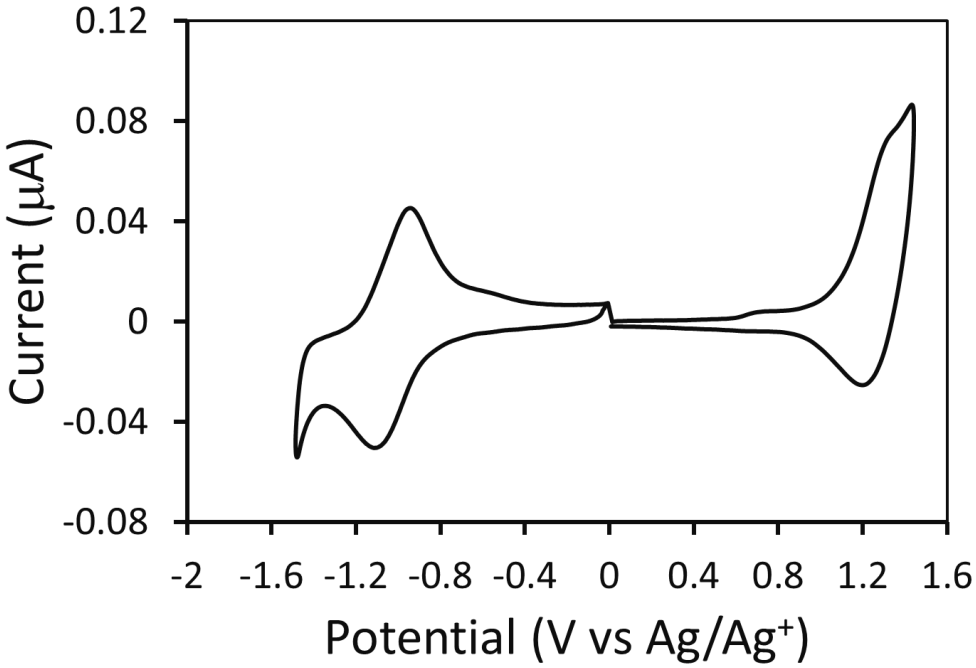

Figure S5. CV plots of the**P(BDTPtQD)**.

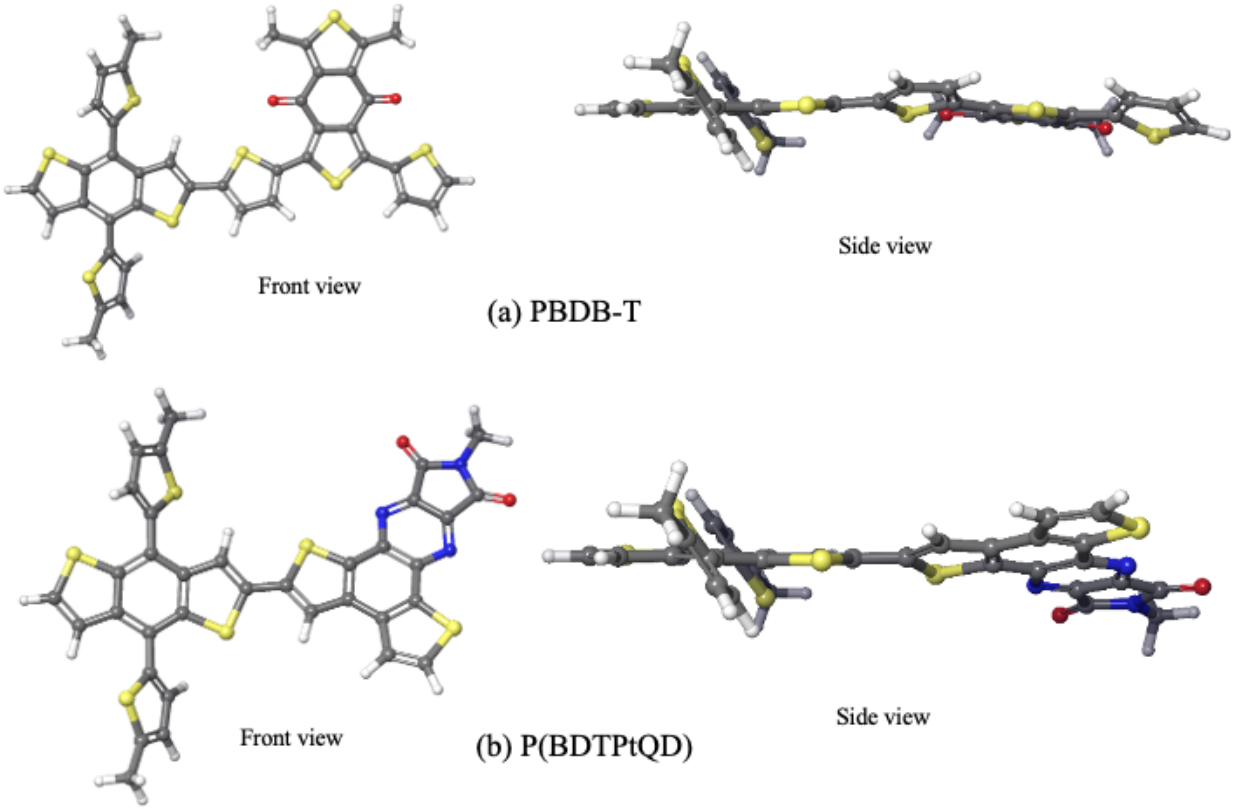

Figure S6.Model of monomer unit (a) PBDB-T and (b)**P(BDTPtQD)** in ground state front view and side view geometry optimized by DFT/PW6B95-D3 (BJ)/6-31G*+

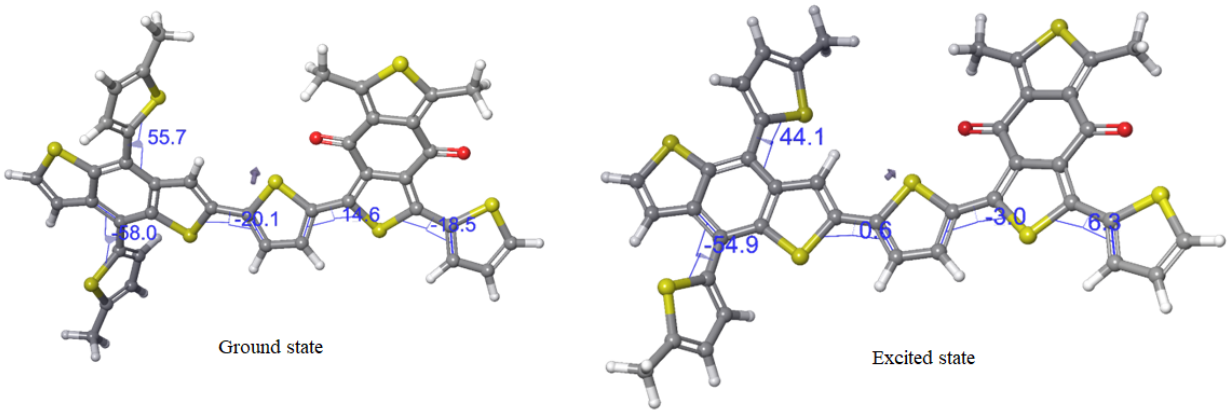

Figure S7. model of monomer unit **P(BDTPtQD)** in ground state, and excited state, geometry optimized by DFT/PW6B95-D3 (BJ)/6-31G*+, torsional angles and dipole moments.

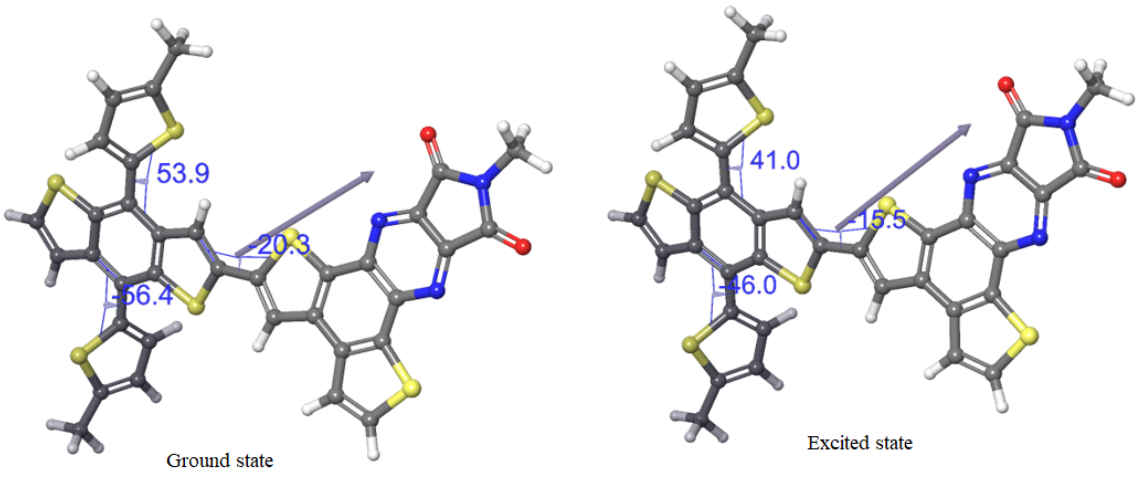

Figure S8. Model of monomer unit **P(BDTPtQD)**in ground state and excited state. Geometry optimized by DFT / PW6B95-D3(BJ) / 6-31G*+. Torsional angles and dipole moment

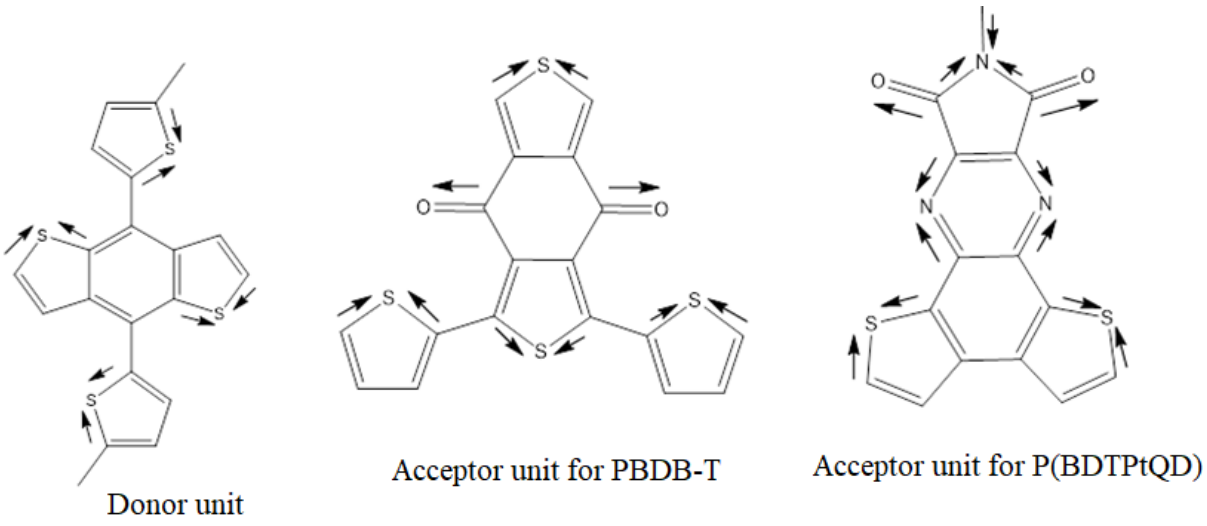

Figure S9. Vector analysis for dipole moment

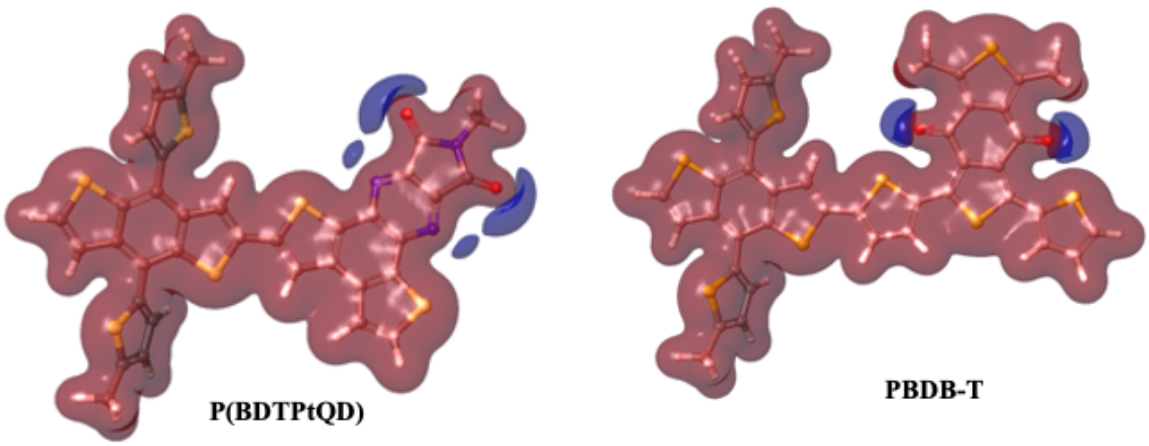

FigureS10. Electrostatic potential surface for the **P(BDTPtQD)** and PBDB-T model. Calculation by method DFT / M11-L / def2-SVPD in acetonitrile (PBF solvent model).

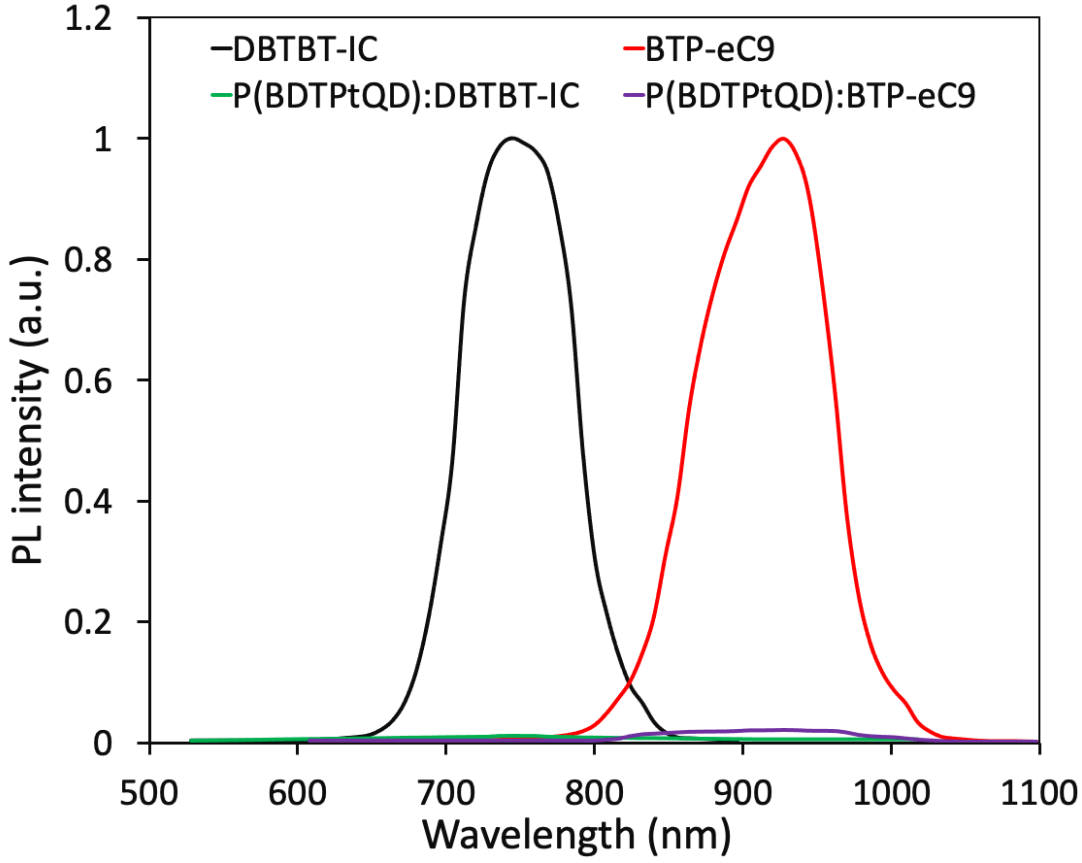

Figure S11. Thin film PL spectra of pristine DBTBT-IC and BTP-eC9 and their blends with **P(BDTPtQD)**, excitation wavelength for DBTBT-IC and BTP-eC9 are 680 nm and 810 nm, respectively.

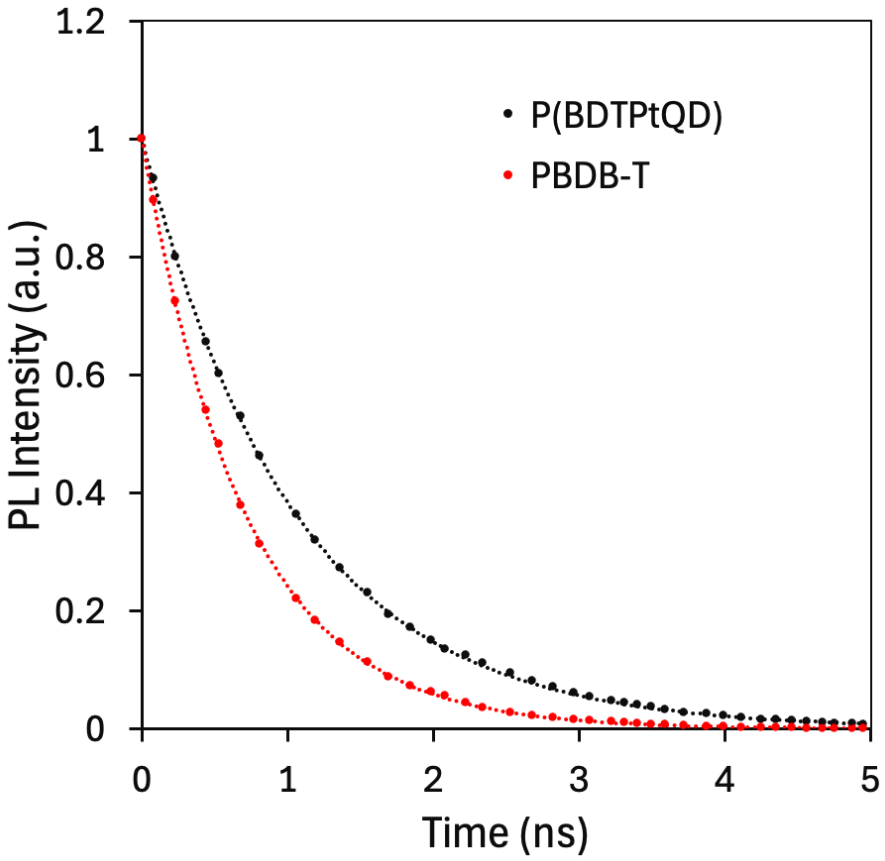

Figure S12. Thin film TRPL spectra of pristine **P(BDTPtQD)** and PBDB-T.

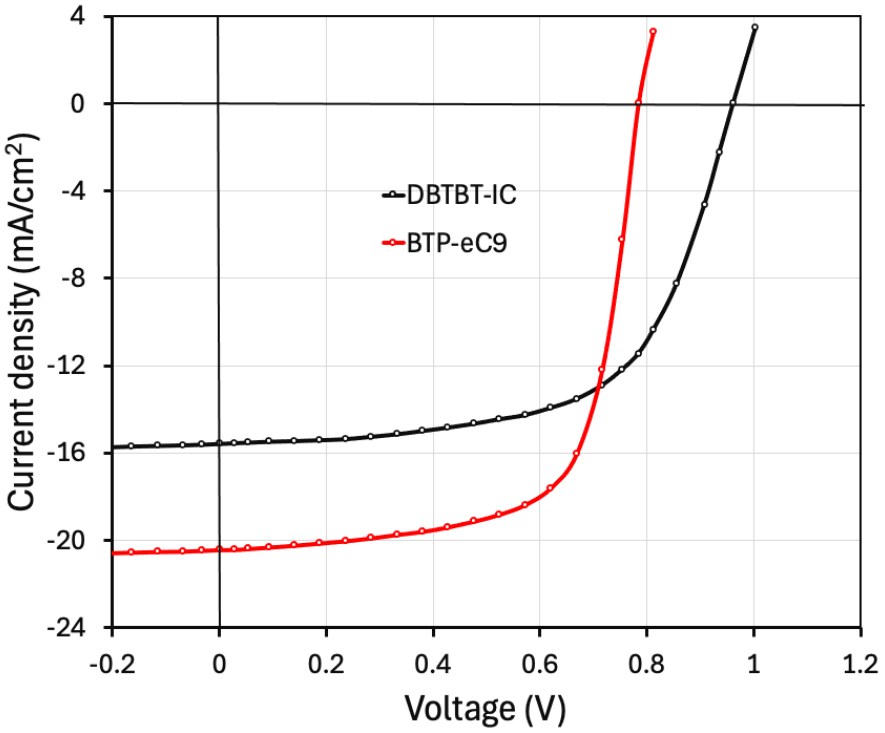

Figure S13. J-V characteristics under illumination (AM1.5, 100 mW/cm$_2$) for OSCs based on SVA treated PBDB-T:DBTBT-IC (1:1.2) and PBDB-T:BTP-eC9 (1:1.2) active layer.

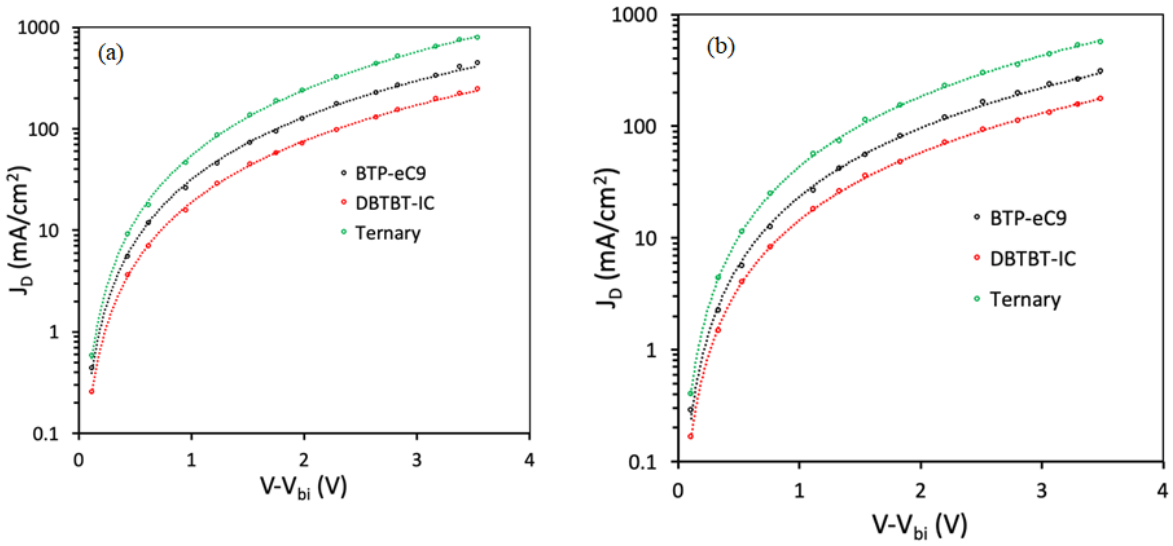

Figure S14. Dark J-V plots and their SCLC fitting for (a) hole-only and (b) electron-only devices.

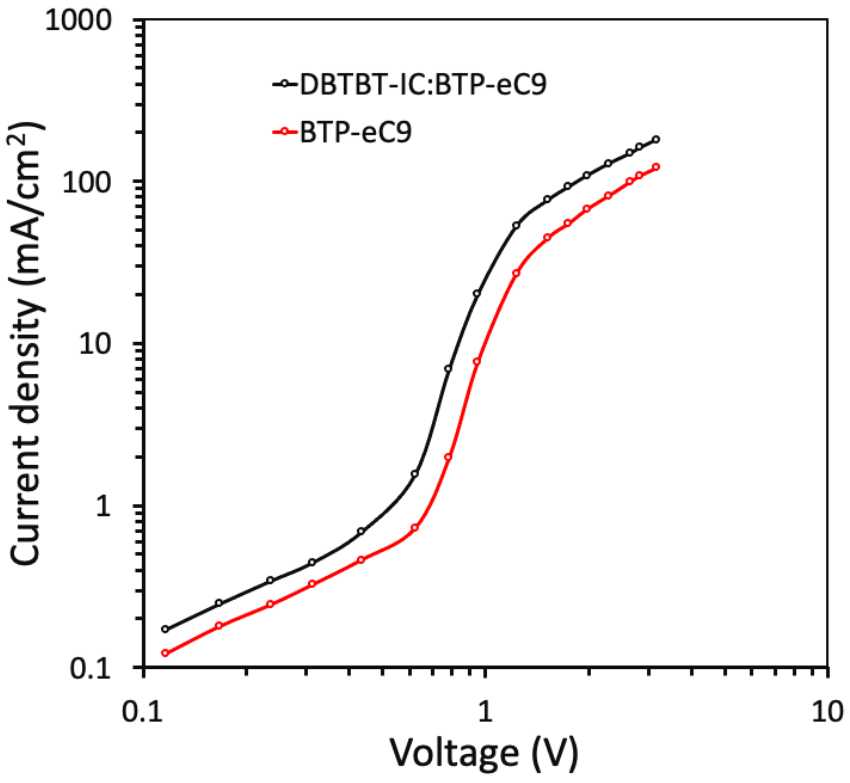

Figure S15. Dark J-V curves to estimate the trap densities in the binary and ternary active layer.

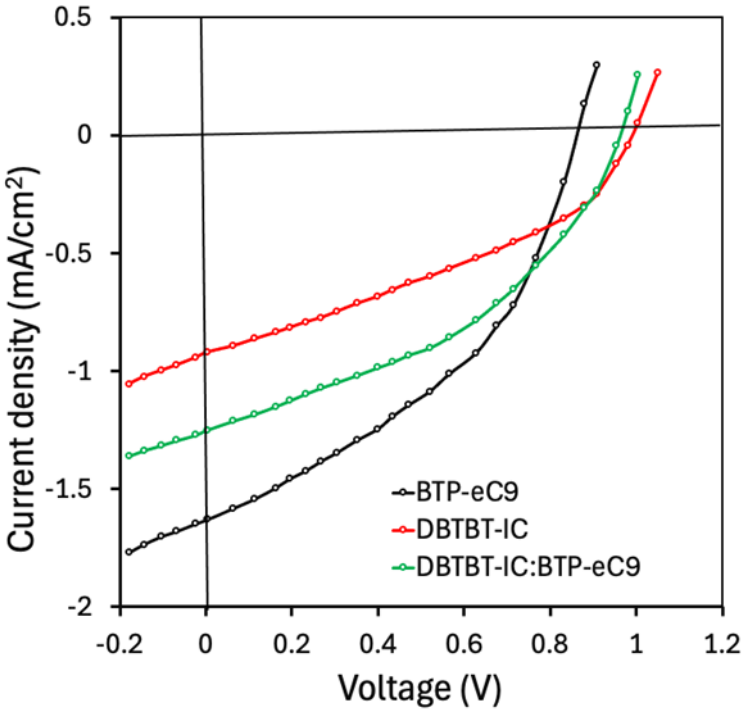

Figure S16. J-V characteristics under illumination for the devices based on BTP-eC9, DBTBT-IC and DBTBT-IC:BTP-eC9 active layers.

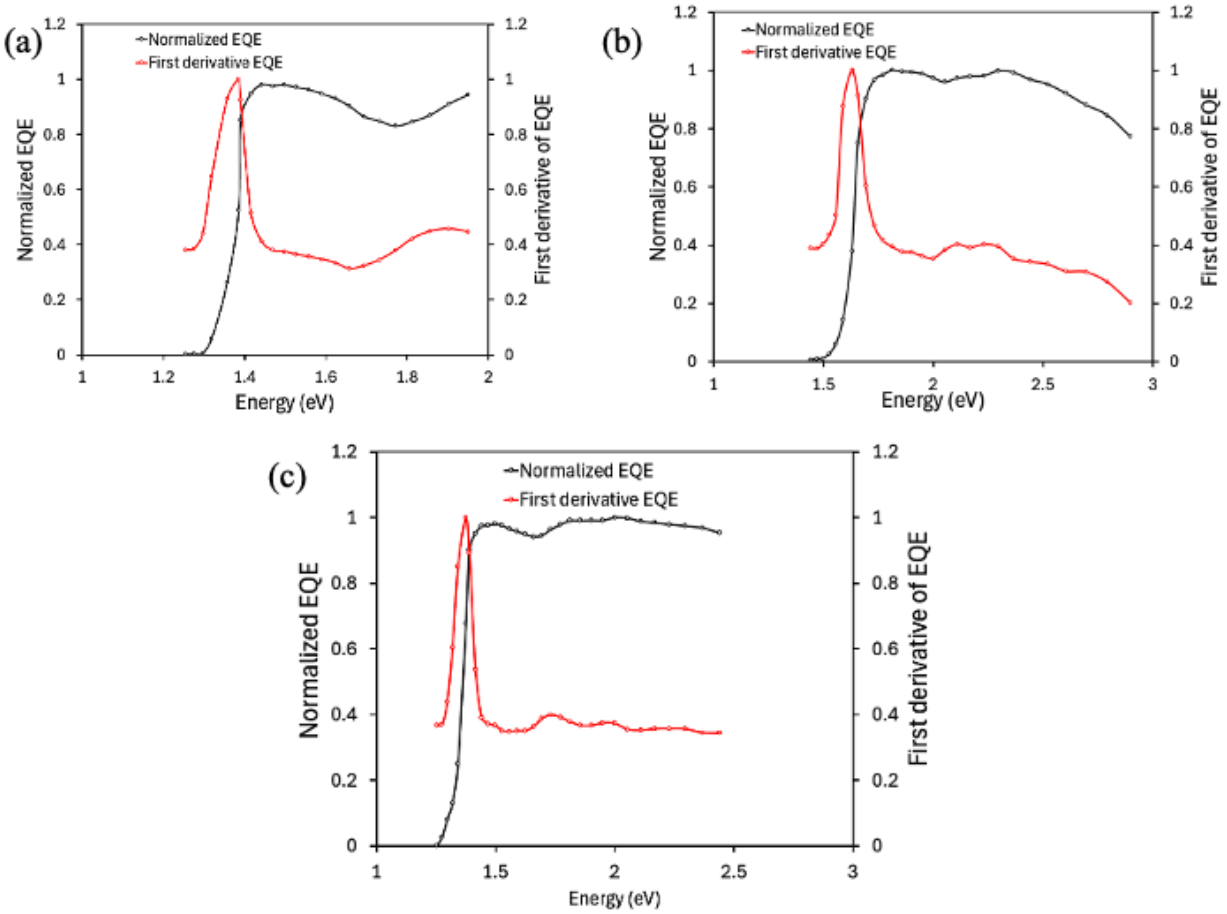

Figure S17. Normalized EQE and first derivatives of EQE plots for (a) **P(BDTPtQD):**BTP-eC9, (b) **P(BDTPtQD)**:DBTBT-IC and (c) **P(BDTPtQD)**:DBTBT-IC:BTP-eC9devices.

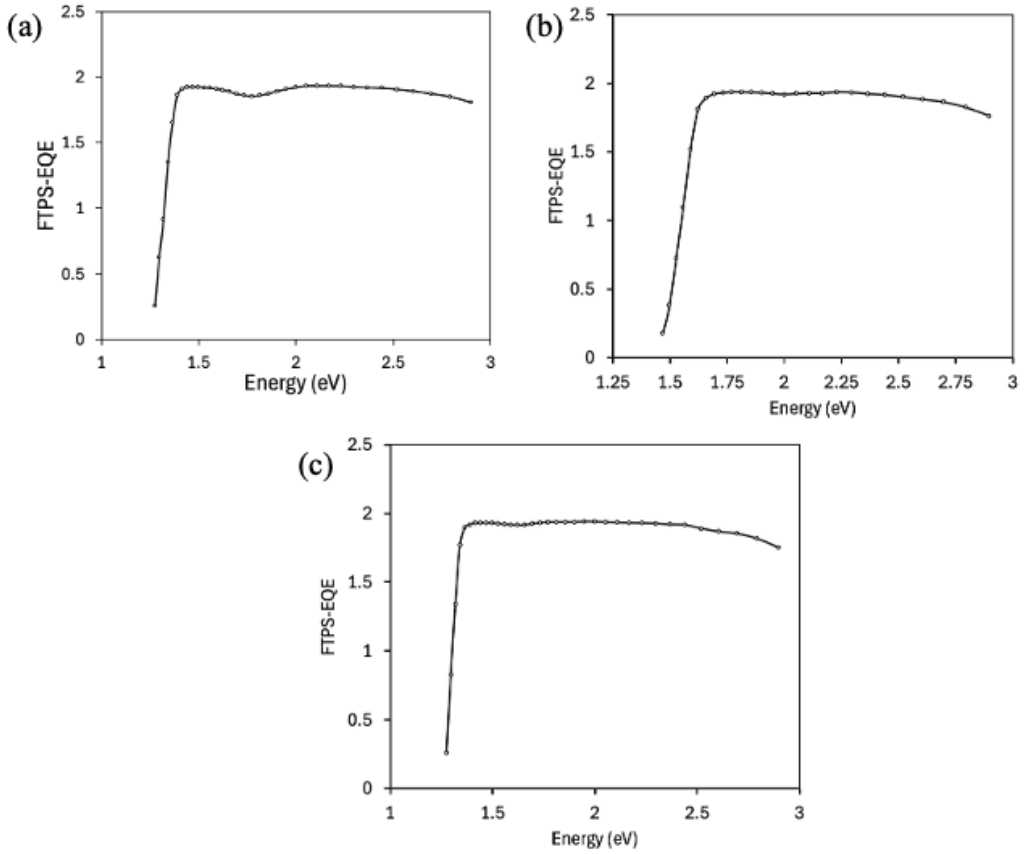

Figure S18. FTPS-EQE plots for (a) **P(BDTPtQD):**BTP-eC9, (b) **P(BDTPtQD)**:DBTBT-IC and (c) **P(BDTPtQD)**:DBTBT-IC:BTP-eC9devices.

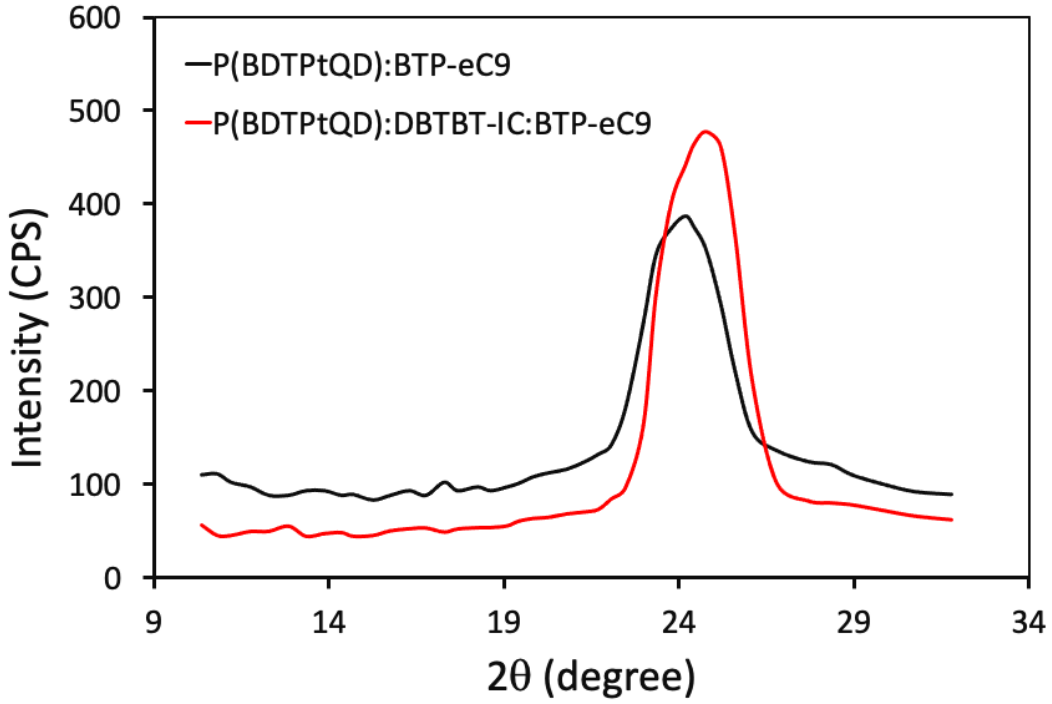

Figure S19. X-ray diffraction patterns in OOP mode for binary and ternary films.

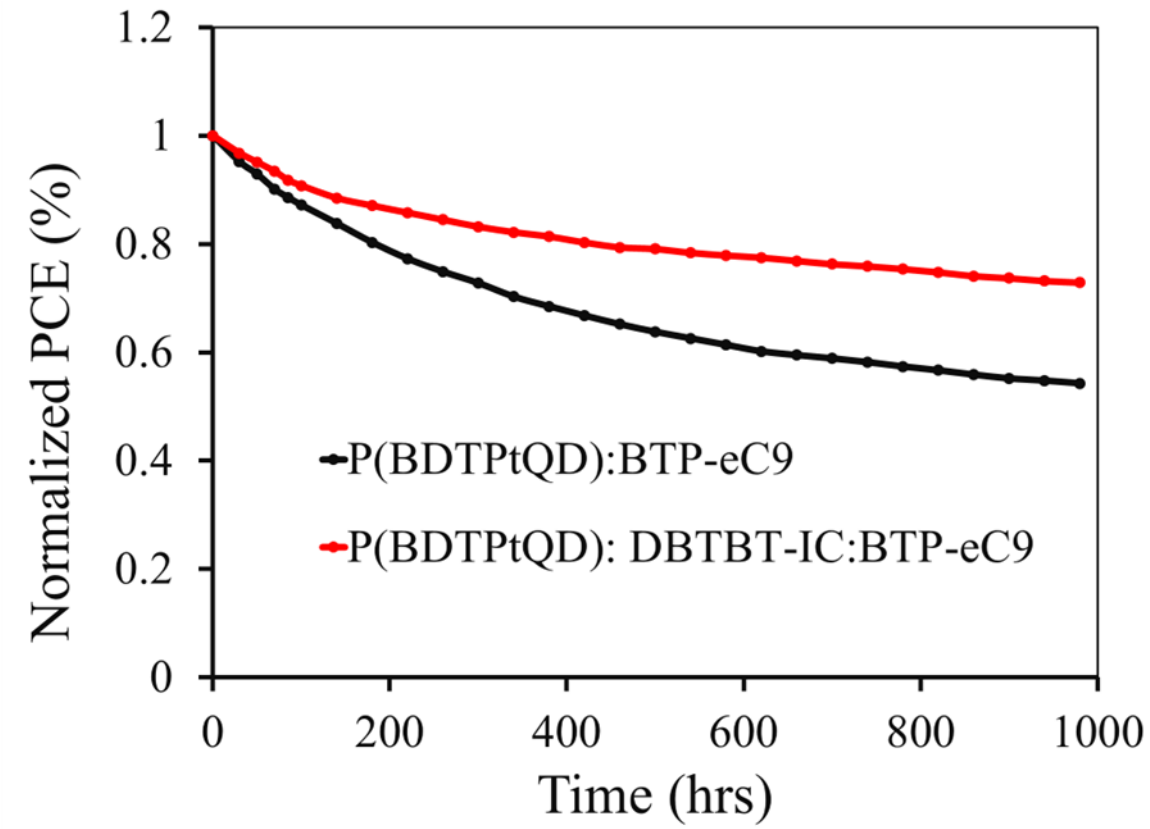

Figure S20. Stability test of the OSCs based on ternary and binary active layers, under ambient conditions.

Table S1a. Photovoltaic parameters of as devices based on as cast **P(BDTPtQD)**:BTP-eC9 with different weight ratios of **P(BDTPtQD)** and BTP-eC9, using chloroform as processing solvent.

Weight ratio	J_{SC} (mA/cm^2)	V_{OC} (V)	FF	PCE (%)
1:0.2	14.86	0.91	0.593	8.02
1:0.8	16.43	0.91	0.618	9.24
1:1.2	**17.56**	**0.90**	**0.643**	**10.17**
1:1.4	16.84	0.90	0.632	9.58

Table S1b. Photovoltaic parameters of as-cast devices based onas-cast **P(BDTPtQD)**: DBTBT-IC with different weight ratios of **P(BDTPtQD)**and DBTBT-IC, utilizing chloroform as processing solvent.

Weight ratio	J_{SC} (mA/cm^2)	V_{OC} (V)	FF	PCE (%)
1:0.2	10.43	1.08	0.563	6.34
1:0.8	12.82	1.09	0.598	8.36
1:1.2	**13.86**	**1.09**	**0.612**	**9.24**
1:1.4	13.32	1.08	0.602	8.66

Table S2. Photovoltaic parameters of OSCs based on SVA-treated PBDB-T:BTP-eC9 (1:1.2) and PBDB-T:DBTBT-IC (1:1.2) active layers.

Active layer	J_{SC} (mA/cm^2)	V_{OC} (V)	FF	PCE (%)

PBDB-T:BTP-eC9	20.43	0.784	0.675	10.81 %
PBDB-T:DBTBT-IC	15.56	0.962	0.654	9.79%

Table S3. Photovoltaic parameters of as-cast ternary devices with different weight ratios of DBTBT-IC and BTP-eC9, and the concentration of **P(BDTPtQD)**is constant, using chloroform as processing solvent.

Weight ratio between DBTBT-IC and BTP-eC9	J_{SC} (mA/cm^2)	V_{OC} (V)	FF	PCE (%)
0.1:1.1	14.84	0.98	0.623	9.06
0.2:1.0	**19.32**	**0.99**	**0.668**	**12.77**
0.4:0.8	17.56	1.0	0.653	11.47

References

1. Cui, R.; Zou, Y.; Xiao, L.; Hsu, C. S.; Keshtov, M. L.; Godovsky, D. Y.; Li, Y. Efficient Solar Cells Based on a New Polymer from Fluorinated Benzothiadiazole and alkylthienyl substituted thieno[2,3-f]benzofuran. *Dyes and Pigments***2015**, *116*, 139-145

2. Keshtov, M.L.; Kuklin, S.A.; Chen, F.C.; Khokhlov, A.R.; Peregudov, A.S.; Siddiqui, S.A.; Sharma G.D.TwoNew D–A Conjugated Polymers P(PTQD-Th) and P(PTQD-2Th) with Same 9-(2-octyldodecyl)-8H-pyrrolo[3,4-b]bisthieno[2,3-f:30 ,20 -h] quinoxaline-8,10(9H)-dioneAcceptor and Different Donor Units for BHJ Polymer Solar Cells Applications. *Org. Electron*. **2015**, *24*, 137-146